JOURNAL OF AGRICULTURAL AND FOOD CHEMISTRY
ARTICLE

J. Agric. Food Chem. 2010, 58, 4537–4544 4537
DOI:10.1021/jf904554s

Detection of Melamine in Milk Powder and Human Urine

Tsung-Hsuan Tsai, Soundappan Thiagarajan, and Shen-Ming Chen*

Electroanalysis and Bioelectrochemistry Laboratory, Department of Chemical Engineering and Biotechnology, National Taipei University of Technology, No. 1, Section 3, Chung-Hsiao East Road, Taipei 106, Taiwan, Republic of China

Detection of melamine has been developed by employing oxidized polycrystalline gold electrode (poly GE). The poly GE was directly utilized for the detection of melamine using differential pulse voltammetry (DPV) and impedimetry. Poly GE successfully showed the oxidation peak for melamine adsorption at 1.1 V is purely based on the detection of adsorption signals of melamine at the electrode surface. Furthermore, the melamine adsorbed poly GE surface has been studied using atomic force microscopy (AFM). Poly GE successfully detects the oxidation signals of melamine in the linear range of 0.05−1.31 ppm in laboratory samples. The proposed poly GE successfully detects the melamine signal (0.06−0.85 ppm) in tainted milk powder samples. It also exhibits two well-separated anodic oxidation peaks for urine and melamine in melamine-spiked human urine samples. Gas chromatography−mass spectrometry (GC-MS) was also employed for the successful detection of melamine in the above proposed real samples.

KEYWORDS: Polycrystalline gold electrode; melamine; cyclic voltammetry; GC-MS; differential pulse voltammetry; milk powder; human urine

INTRODUCTION

Melamine is an organic base and known as a trimer of cynamide with a 1,3,5-triazine skeleton that contains 66% nitrogen by mass. Because of its nitrogen content, it has fire retardant properties. Thus, it has been used as a fire retardant in industries. The combination of melamine with formaldehyde resulted in melamine resin, used in thermosetting plastic, foam, and polymeric products. It also utilized to produce superplasticizers and high-resistance concretes. Melamine adulteration in animal feeds and milk powders is well-known. Due to its very high proportion of nitrogen, melamine has been added illegally to foods and feeds to increase the measured protein content, which determines the value of the product.

Some analysis methods for the determination of protein content actually measure the amount of nitrogen content present in the samples. Therefore, the significant amount of nitrogen content in the samples will indicate that the sample is enriched with higher protein contents. Therefore, melamine has been added to milk powders to increase their protein content. This scientific scandal resulted in protein-enriched milk powders being discovered in laboratory analysis, which resulted in high sales of the milk products. Initially, this type of scandal came to light because in 2007 melamine was found in animal feeds, which caused serious illness and death in animals. Recently, the melamine scandal in milk powder came to light in September 2008 in China. Fresh milk, powdered formula, and other milk-related bakery products are also well-known for melamine scandals (*1*). Melamine-tainted milk consumption has created renal stones and hemeaturia in children and finally acute renal failure (*2*). Thus, there is an immediate urgency to develop an easy and convenient method for the detection and determination of melamine.

Previously, the detection and estimation of melamine were done by utilizing different types of analytical techniques. Some important literature reports are melamine detection using wet-strength paper by ultraviolet spectrophotometry (*3*); detection of urea, melamine, isocyanate, and urethane resins (*4*); determination of melamine in muscle tissue by liquid chromatography−tandem mass spectrometry (*5*); high-performance liquid chromatographic method for the simultaneous detection of the adulteration of cereal flours with melamine and related triazine byproducts ammeline, ammelide, and cyanuric acid (*6*); validation of melamine and its derivatives in rice concentrates using liquid chromatography and its application to animal feed samples (*7*); determination of melamine derivatives, melame, meleme, ammeline, and ammelide by high-performance cation-exchange chromatography (*8*); high-performance liquid chromatographic determination of cyromazine and its derivative melamine in poultry meats and eggs (*9*); residue determination of cyromazine and its metabolite melamine in chard samples by ion-pair liquid chromatography coupled to electrospray tandem mass spectrometry (*10*); determination of cyromazine and melamine residues in soil using liquid chromatography−ultraviolet visible spectroscopy and gas chromatography−mass selective detection (*11*); detection of melamine in gluten, chicken feed, and processed foods using surface-enhanced Raman spectroscopy and high-performance liquid chromatography (*12*); and analysis of melamine−formaldehyde resins by capillary zone electrophoresis−mass spectrometry using ion-trap and quadrupole-time-of-flight mass spectrometers (*13*)

*Corresponding author [e-mail smchen78@ms15.hinet.net; telephone (+886)-2-27712171-2552; fax (+886)-2-27025238].

Published on Web 03/30/2010

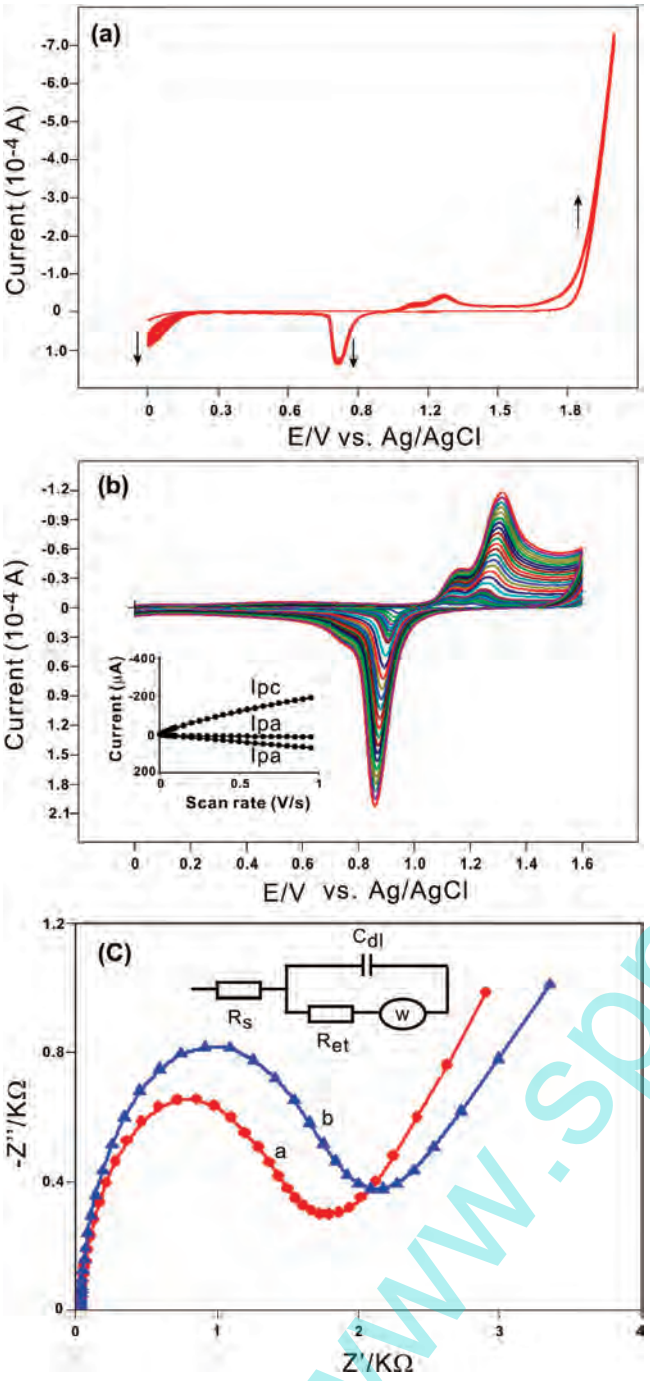

Figure 1. (**a**) Cyclic voltammograms of GE in 0.1 M H_2SO_4 (scan rate = 0.1 V/s). (**b**) Cyclic voltammograms of poly GE in 0.1 M H_2SO_4 (scan rate = 0.01−1 V/s). (Inset) Cathodic (I_{pc}) and anodic peak currents (I_{pa1}, I_{pa2}) of poly GE versus scan rate. (**c**) Electrochemical impedance spectra curves of (a) bare GE and (b) poly GE in 5 mM $[Fe(CN)_6]^{3-/4-}$ in 0.1 M H_2SO_4 (pH 1.0). (Inset) Simple Randles circuit model for the proposed poly GE.

and by capillary zone electrophoresis with electrospray ionization mass spectrometric detection (*14*).

Adsorption of organics on gold electrodes is found as a special topic in the field of electrochemistry. Especially, modifications on the polycrystalline gold electrode (poly GE) surface resulted in various types of applications. For example, the adsorption of pyridine (*15*), electrochemical reactions of ethyne adsorption (*16*), and direct electrochemical oxidation of DNA on poly GE have been reported (*17*). Sulfur-containing thiol group interaction with gold electrode also resulted in different types of electrode modification processes in the field of electroanalytical chemistry. There also some interesting reports on the self-assembly of melamine structures on gold surfaces. A few examples are the theoretical study of melamine superstructures and their interaction with the Au (111) surface (*18*), bimolecular networks and supramolecular traps on Au (111) (*19*), hierarchical organization on a two-dimensional supramolecular network (*20*), and melamine structures on the Au (111) surface (*21*). Thus, on the basis of these previous literature reports, we employed the poly GE for the detection of adsorbed melamine using differential pulse voltammetry (DPV) and impedimetric techniques. The proposed poly GE was found to be sensitive for the detection of melamine in the parts per million range. The poly GE was also sensitive for the detection of melamine in tainted milk powders and human urine samples in the parts per million range.

EXPERIMENTAL PROCEDURES

Materials. Melamine was purchased from Chem Service Inc., West Chester, PA. All other chemicals (Merck) used in this investigation were of analytical grade (99%). Double-distilled deionized water was used to prepare all of the solutions. Melamine was dissolved in 0.1 M H_2SO_4 (pH 1) for all of the electrochemical studies. Pure nitrogen was passed through all of the experimental solutions. Banned melamine-tainted milk powder was directly employed for the real sample analysis: 1.428 g of melamine-tainted milk powder was dissolved in 25 mL of 0.1 M H_2SO_4, and the mixture was placed in an ultrasonication bath for about 10 min to obtain a homogeneous sample. Human urine samples have been obtained from a single donor.

Measurements and Apparatus. All of the electrochemical experiments were performed using a CHI 1205a electrochemical workstation (CH Instruments, Austin, TX). A conventional three-electrode system, which consists of Ag/AgCl saturated with 3 mol L^{-1} KCl as a reference electrode, bare or oxidized polycrystalline gold electrode (poly GE) as working electrode, and platinum wire as counter electrode, was used for all of the electrochemical experiments. The GE ($\varphi = 0.3$ cm in diameter) was obtained from Bioanalytical Systems, Inc., West Lafayette, IN). All of the experiments were conducted at room temperature. Electrochemical impedance studies (EIS) was performed by using a Zahner impedance analyzer (Zahner Elektrik Gmbh & Co. KG, Kronach, Germany). Electrochemical quartz crystal microbalance (EQCM) experiments were done by using CHI 410a potentiostats (CH Instruments). The working electrode for EQCM measurements was an 8 MHz AT-cut quartz crystal coated with gold. The diameter of the quartz crystal was 13.7 mm; the gold electrode diameter was 5 mm. The AFM images were recorded with a multimode scanning probe microscope system operated in tapping mode using Being Nano-Instruments CSPM-4000, Ben Yuan Ltd. (Beijing, China). The real samples have been analyzed by using an Agilent 6890N/5975 GC/MS (Agilent, Palo Alto, CA). Gas chromatographic separations were performed using a 30 m DB-5 ms capillary column (0.25 mm i.d., 0.25 μm). Injection volume was 1 μL.

Fabrication and Characterization of Poly GE. Prior to the electrooxidation process, the GE was well polished with the help of a BAS polishing kit with aqueous slurries of alumina powder (0.05 μm), rinsed, and ultrasonicated in double-distilled deionized water. Then the GE surface was oxidized by performing 10 cycles in 0.1 mol L^{-1} H_2SO_4 between 0 and 2 at 0.1 V s^{-1} (**Figure 1a**).

RESULTS AND DISCUSSION

Characterization of Poly GE. The oxidized poly GE surface was again washed with deionized water and transferred to 0.1 mol L^{-1} H_2SO_4 (pH 1) solutions for the electrocatalytic reactions. The poly GE was employed for different scan rate studies in 0.1 M H_2SO_4. **Figure 1b** exhibits different scan rate studies of poly GE in the range of 0.01−1 V/s. This study clearly shows that for the increasing scan rates the reduction (at 0.9 V) and oxidization peak currents (at 1.13 and 1.24 V) (*22*−*24*) increase and both the oxidation and reduction peaks of poly GE shift to more negative and positive potentials at the higher scan rates. The anodic and

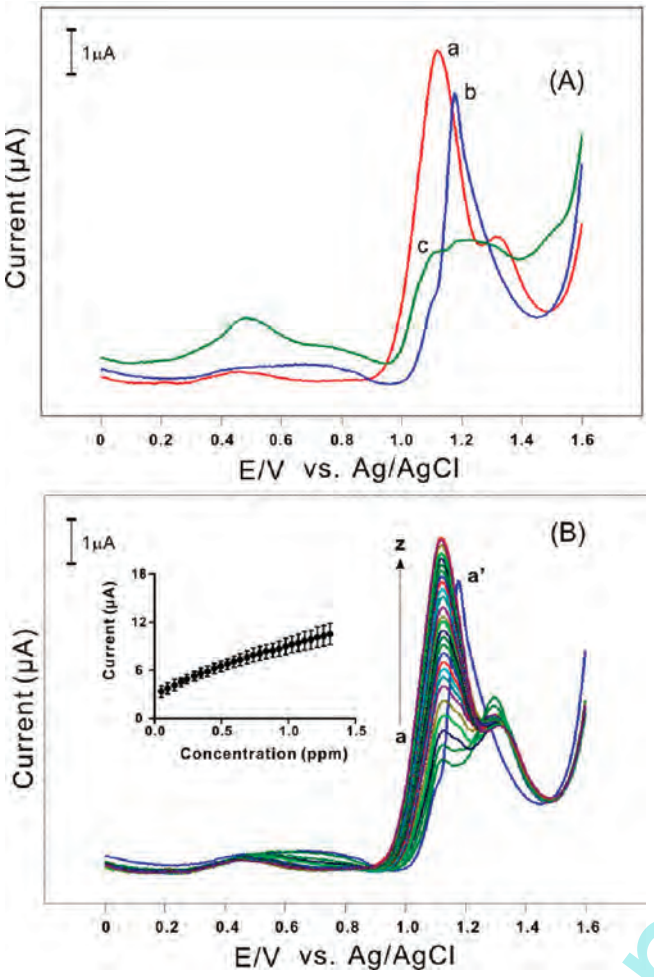

Figure 2. (**A**) DPVs signal of melamine on (a) poly GE (1.311 ppm), (c) bare GE (1.311 ppm), and (b) DPV of poly GE in the absence of melamine in 0.1 M H_2SO_4 (pH 1). (**B**) DPV signals of melamine detection in 0.1 M H_2SO_4 (pH 1) on poly GE. Melamine concentrations were 0, 0.05, 0.09, 0.14, 0.19, 0.24, 0.29, 0.34, 0.39, 0.44, 0.49, 0.54, 0.59, 0.64, 0.68, 0.73, 0.78, 0.83, 0.88, 0.93, 0.97, 1.02, 1.07, 1.12, 1.16, 1.21, 1.26, and 1.31 ppm. (Inset) Calibration plot of melamine detection (n = 5).

cathodic peak currents were linearly dependent on the scan rate, indicating that the poly GE surface reaction was a surface-controlled process. The inset of **Figure 1b** shows the anodic (I_{pa}) and cathodic currents (I_{pc}) versus the scan rate. The linear increase in the peak current of both anodic and cathodic peaks shows that the poly GE has linear dependency with respect to the scan rate. The linear regression equations for the both anodic and cathodic peaks were respectively expressed as I_{pa1} (μA) = 0.072v (V/s) + 1.249, R^2 = 0.999, I_{pa2} (μA) = 0.009v (V/s) + 3.847, R^2 = 0950, and I_{pc} (μA) = −0.190v (V/s) − 14.69, R^2 = 0.989.

Poly GE was examined using electrochemical impedance spectroscopic analysis. Electrochemical impedance spectra are commonly examined by using an equivalent circuit model, which fits and relates to a distinct physiochemical process. In this, the Nyquist plot of electrochemical impedance spectra shows the exact electron-transfer resistance nature of the films. As shown in **Figure 1c**, curve a indicates the Nyquist plot of bare GE and curve b shows the poly GE in the presence of 5 mM $[Fe(CN)_6]^{3-/4-}$ in 0.1 M H_2SO_4 (pH 1.0). The impedance spectra curves in **Figure 1c** exhibit as a semicircle ending with a linear straight line, which corresponds to the electron-transfer and the diffusion process, respectively. The respective semicircle parameters correspond to the electron-transfer resistance (R_{et}) and the double layer capacity (C_{dl}). As shown in **Figure 1c**, for bare GE (curve a) the semicircle area (R_{et} = 1.725 KΩ) is smaller, which indicates a very low electron-transfer resistance nature of the electrode (C_{dl} = 0.2048 pF, solution resistance (R_s) = 0.0313 KΩ). At the same time, after the oxidation process, the poly GE exhibits a higher value of electron-transfer resistance (curve b, R_{et} = 1.999 KΩ) (C_{dl} = 0.2066 pF, R_s = 0.0292 KΩ). This shows that the surface of the GE has been modified with polycrystalline nature, which makes the electron-transfer kinetics process a slower one. We have applied a simplified Randles circuit model (Warburg element (w)), which has been used to fit the impedance spectra. The inset in the **Figure 1c** shows the simplified Randles circuit, which was well suited with the impedance spectroscopic results. From this Nyquist plot (**Figure 1c**) the electrochemical behavior of the poly GE surface has been authenticated.

Differential Pulse Voltammetric Detection of Melamine. The proposed poly GE was employed for the detection of melamine. **Figure 2A**, curve a, show the differential pulse voltammogram of poly GE immersed in 0.1 M H_2SO_4 (pH 1) containing 1.311 ppm melamine. The adsorbed melamine oxidation signal appears at 1.11 V. At the same time, curve b shows the oxidation signal for poly GE (at 1.17 V) in the absence of melamine in 0.1 M H_2SO_4. Polished bare GE displays a diminished oxidation peak for 0.1 M H_2SO_4 containing 1.31 ppm melamine at 1.2 V. Comparing the DPV curves b and a of **Figure 2A**, we can clearly conclude that the oxidized poly GE adsorbs the specific amount of melamine which resulted to show its oxidation peak around 1.11 V, respectively. At the same time, bare GE fails to show the significant response for melamine detection and shows only a broad diminished peak around 1.2 V. Thus, the voltammetric response with the potential shift (**Figure 2A**, curve a) strongly indicates that the adsorption of melamine occurred on the poly GE surface. Poly GE also exhibits a small oxidation peak around 1.34 V, which is not significant, and the peak current diminishes for the continuous increasing concentrations of melamine. The melamine adsorption on the poly GE surface results in the electrode surface site blocking results in the slow electron-transfer process on the electrode surface. Also, the continuous adsorption of melamine does not result in the entire electrode surface blocking; however, still, as discussed before, it only makes the electron-transfer process as a slower one.

Further examination was made with the continuous addition of melamine in 0.1 M H_2SO_4. **Figure 2B** shows the continuous electrocatalytic oxidation peaks of adsorbed melamine on the poly GE surface. The melamine has been added in the concentration ranges of 0.05−1.31 ppm. As discussed before, the poly GE electrode clearly exhibits the oxidation peak of adsorbed melamine at 1.11 V. For the continuous addition of melamine, the poly GE shows a sharp oxidation peak (1.11 V) and a second peak around 1.3 V, which does not increase for the increasing concentrations of melamine. Thus, we concluded that the peak obtained at 1.11 V originates for the detection of adsorbed melamine. For the increasing concentrations, melamine has been adsorbed on the poly GE surface; the peak current sharply diminishes and finally attains a saturated limit of adsorption, respectively.

This result validates that the proposed electrode possesses a certain linear range of detection (approximately 0.05−1.31 ppm) for the melamine detection. Curve a′ shows the DPV response of anodic oxidation current of poly GE in 0.1 M H_2SO_4. Comparing this curve a′ with the electrocatalytic curves of melamine detection, we can conclude that the increasing electro-oxidation signals are due to the adsorption of melamine on poly GE. However, at the beginning, on the addition of first concentration, the anodic catalytic current for the melamine decreases at the initial

concentration and increases linearly for the increasing concentrations, respectively. Therefore, at the beginning, the adsorption of melamine on poly GE prevents the exhibition of the anodic oxidation current of poly GE and increases with respect to the increasing concentrations of melamine. These results clearly validate the suitability of poly GE for the melamine detection process. On the basis of the previous literature, the aim of the proposed work was to detect the melamine in parts per million, which absolutely fits for the proposed electrode. The inset of **Figure 2B** shows the current versus calibration plot for the melamine detection. Each addition of melamine concentration has been examined for $n = 5$ times and plotted in the calibration plot. From the calibration plot, the linear regression equation for the detection of melamine ($n = 5$) was found as current I_{pa} (μA) = 5.509C (ppm) + 3.5542, with the correlation coefficient of $R^2 = 0.990$.

Impedimetric Detection of Melamine on Poly GE. Figure 3 show the Nyquist curves obtained for the adsorption of melamine at the poly GE. The plot of the real component (Z') and the imaginary component Z'' (imaginary) resulted in the formation of a semicircular Nyquist plot. This type of impedance spectrum is an analytic of a surface-modified electrode system in which the electron transfer is slow and the impedance is controlled by the interfacial electron transfer at high frequency. Open circuit potential was applied for this investigation. The concentrations of added melamine were in the range of 0−0.93 ppm. The electron-transfer resistance (R_{et}) changes from the baseline response for each addition of melamine.

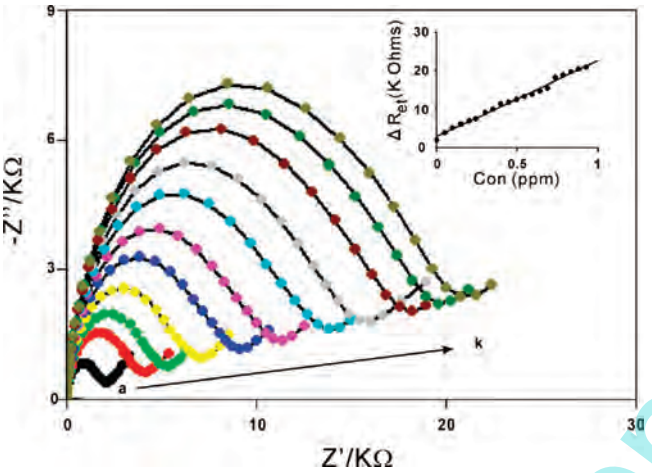

Figure 3. Nyquist plot response of poly GE for the various concentrations of melamine in 5 mM $[Fe(CN)_6]^{3-/4-}$ in 0.1 M H_2SO_4 (pH 1.0). The melamine concentrations were (a−k) 0, 0.05, 0.09, 0.19, 0.29, 0.39, 0.59, 0.68, 0.73, 0.83, and 0.93 ppm, respectively. (Inset) Calibration plot of ΔR_{et} versus concentration of melamine (ppm) for melamine detection on poly GE.

Particularly the insulation property of the poly GE increases upon adsorption of melamine, which hinders the electron-transfer kinetics at the poly GE surface. The electron-transfer resistance increases with the increasing concentrations of melamine, which gives rise to a linear-type detection response from 0.5 to 0.93 ppm. For 0.73 and 0.93 ppm concentrations, the curve begins to come closer, which suggests that the poly GE surface approaches the saturation limit for the adsorption of melamine. Several models were attempted, and the best fit for the data has been employed. Up to 0.93 ppm, the experimental data fitted and the regression equation obtained was R_{et} (kΩ) = 19.553C (ppm) + 2.9489 with a correlation coefficient of $R^2 = 0.992$ (inset of **Figure 3**). These results clearly explicate the impedimetric detection of melamine using poly GE.

AFM Analysis of Melamine-Adsorbed GCQ Surface. AFM imaging provides more detailed information about the surface morphology of bare, oxidized, and melamine-adsorbed gold-coated quartz crystal (GCQ) surfaces. For the AFM analysis the gold-coated quartz crystal was oxidized using the same condition to attain the oxidized poly GE surface nature using the EQCM technique, respectively. After this process, a deaerated 0.5 ppm melamine solution in (0.1 M H_2SO_4, pH 1) was employed in the EQCM cell for the self-adsorption of melamine. The EQCM crystal was washed with a copious amount of water, then dried, and examined using AFM. AFM tapping mode has been employed for the electrode surface analysis. **Figure 4** shows typical AFM 2D images of the bare (**a**), oxidized polycrystalline (**b**), and melamine-adsorbed (**c**) GCQ surfaces. In the AFM analysis the bare GCQ exhibited as (**Figure 4a**) a plain smooth surface. At the same time, after the oxidation process, the GCQ

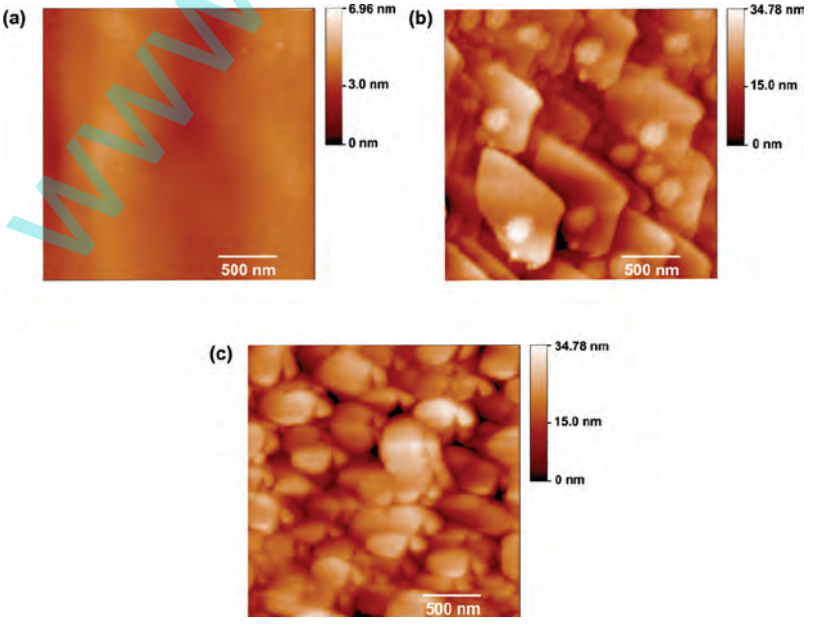

Figure 4. AFM topographic images of (**a**) bare, (**b**) oxidized polycrystalline gold coated quartz crystal electrode (GCQ), and (**c**) melamine-adsorbed poly GCQ.

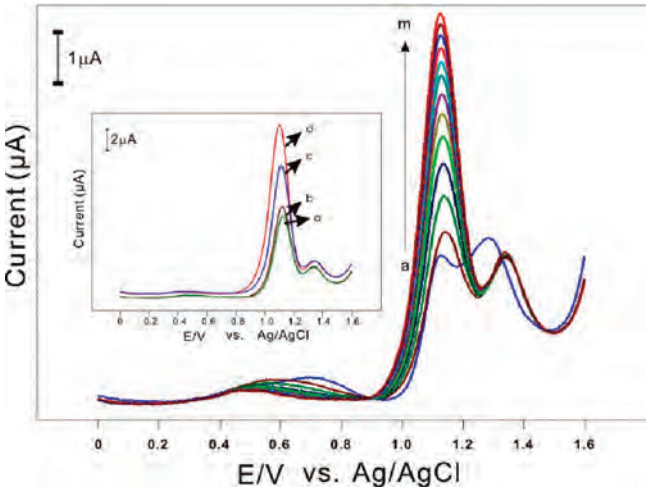

Figure 5. Curves a−m display the DPVs of poly GE for melamine detection in 0.1 M H_2SO_4 solution containing melamine-tainted milk powder (1.428 g, the melamine concentration was reported in the range of 0.06−0.85 ppm, melamine-tainted milk powder and 0.1 M H_2SO_4 solution (pH 1) mixture ratio is 1:3). The concentration mixture added from a to m is 100 μL. (Inset) DPVs of poly GE for melamine detection in various concentration mixture ratios. The concentration mixture ratios are (melamine-tainted milk powder and 0.1 M H_2SO_4 solution (pH 1)) is (a) 1:50, (b) 1:25, (c) 1:10, and (d) 1:3.

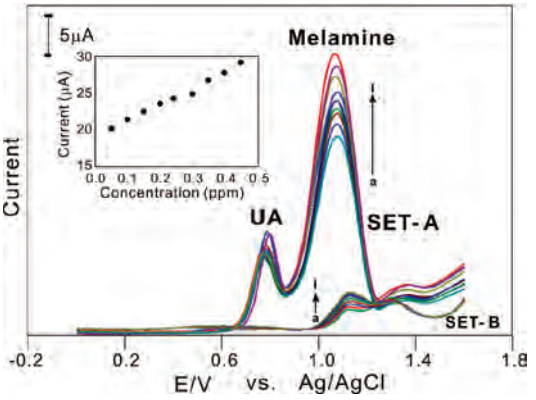

Figure 6. SET-A displays the DPV signals of melamine detection in human urine sample (pH 1) using poly GE. The spiked melamine concentrations in the human urine sample (dissolved in pH 1 H_2SO_4) were (a) 0.05, (b) 0.09, (c) 0.14, (d) 0.19, (e) 0.24, (f) 0.29, (g) 0.34, (h) 0.39, and (i) 0.44 ppm. (Inset) Current versus concentration plot for melamine detection in urine sample. SET-B displays the overlaid DPV signals of melamine detection in pH 1 H_2SO_4 at poly GE. The melamine concentrations (dissolved in pH 1 H_2SO_4) were (a) 0.05, (b) 0.09, (c) 0.14, (d) 0.19, (e) 0.24, (f) 0.29, (g) 0.34, (h) 0.39, and (i) 0.44 ppm.

was scanned again (**Figure 4b**). The oxidized GCQ surface exhibits its own polycrystalline shape structure (small triangular particles). This result validates the oxidized polycrystalline nature of the GCQ surface. **Figure 4c** shows the melamine-adsorbed poly GCQ surface. On the basis of this three AFM 2D image, we can clearly depict the difference between the unmodified, modified, and melamine-adsorbed GCQ surfaces. Also, various AFM parameters have been calculated.

The average roughness (AR) values were obtained using the 2D image topography of bare, oxidized, and melamine-adsorbed GCQ surfaces. The surface roughness value averaged from the images taken with different scan size increases 0.434 nm for an unmodified bare GCQ, 4.43 nm for oxidized poly GCQ, and 4.45 nm for melamine-adsorbed poly GCQ. These values are averages calculated from several images acquired in different regions of the respective samples. Generally, the bare GCQ surface exhibits a very smooth morphology, which can be seen in **Figure 4a** with the root-mean-square roughness (rms) (0.505 nm) being smaller than that of the poly GCQ (5.55 nm) and melamine-adsorbed poly GCQ surface (5.47 nm). Increase of rms roughness of the poly GCQ surface was due to the oxidation process and polycrystalline nature, which naturally increases the surface roughness of the electrode surface. In the AFM parameter analysis, the surface skewness (Sk) depicts the asymmetric nature of the height distribution in the sample. For the poly GCQ surface, the higher negative Sk value (−0.341) has been obtained because the oxidation process results in the GCQ surface with a porous nature comparing with the bare GE (−0.117). At the same time, for melamine-adsorbed GCQ the very low Sk value (−0.0717) indicates the adsorption of melamine on the poly GCQ surface. The surface kurtosis (Ku) value illustrates the sharpness of the surface height distribution. In this, a value that equals 3.0 is found as a Gaussian-like surface. For the oxidized poly GCQ a surface kurtosis value of 3.04 was found compared with the bare GE (2.05) and melamine-adsorbed poly GCQ (2.79). The oxidized poly GCQ surface show a high kurtosis value, and the melamine-adsorbed and bare GCQ show low Ku values, indicating that the oxidized poly GCQ has almost a unique crystalline structure. This AFM result validates the polycrystalline nature and the melamine-adsorbed poly GCQ surface nature, respectively.

Melamine Detection in Tainted Milk Powder Using Poly GE. To evaluate the commercial application of the proposed poly GE, we have examined the melamine-tainted milk samples for real sample analysis. For the melamine-tainted milk powder solution (dissolved in 0.1 M H_2SO_4 (pH 1)) the poly GE shows the oxidation peak of adsorbed melamine around 1.1 V. Previously, the amount of melamine (0.06−0.85 ppm, protein content = 8.5 mg/per glass of 250 mL) present in the tainted milk powder was evaluated using liquid chromatography (LC)−mass spectroscopy (MS)/MS and reported for prevention and public awareness. Thus, we have directly employed the tainted milk powder content for the detection of melamine. For each 100 μL addition of melamine-tainted milk powder solution, the oxidation peak current at the poly GE clearly increased.

This shows that the melamine present in the milk powder has been adsorbed on the poly GE surface. From this result, we can clearly understand that poly GE possesses the nature for the detection of melamine in real milk powder solutions. The inset in **Figure 5** shows the DPVs of melamine-tainted milk powder dissolved in 0.1 M H_2SO_4 in the ratios of (melamine-tainted milk powder/0.1 M H_2SO_4 (pH 1)) 1:50, 1:25, 1:10, and 1:3. For the increasing concentrations of melamine ratio, poly GE clearly shows the sharp anodic oxidation peaks for adsorbed melamine. Thus, this real sample analysis result clearly shows the capability of poly GE for the detection of melamine in tainted milk powder samples in the parts per million range.

Melamine Detection in Human Urine Samples Using Poly GE. Melamine detection has been examined in human urine samples using poly GE. Before the examination, freshly collected human urine sample (pH 6.8) were filtered several times using Whatman filter paper (grade 1). Filtered human urine was centrifuged for 1 h to eliminate the other unwanted precipitates. Then the supernatant sample was filtered again. In the next step, the purified human urine sample was diluted using 0.1 M H_2SO_4 to attain pH 1. After this, the parts per million concentrations (curves a−g) of melamine (dissolved in pH 1 H_2SO_4) have been directly spiked in the prepared human urine sample. **Figure 6**, SET-A, shows the

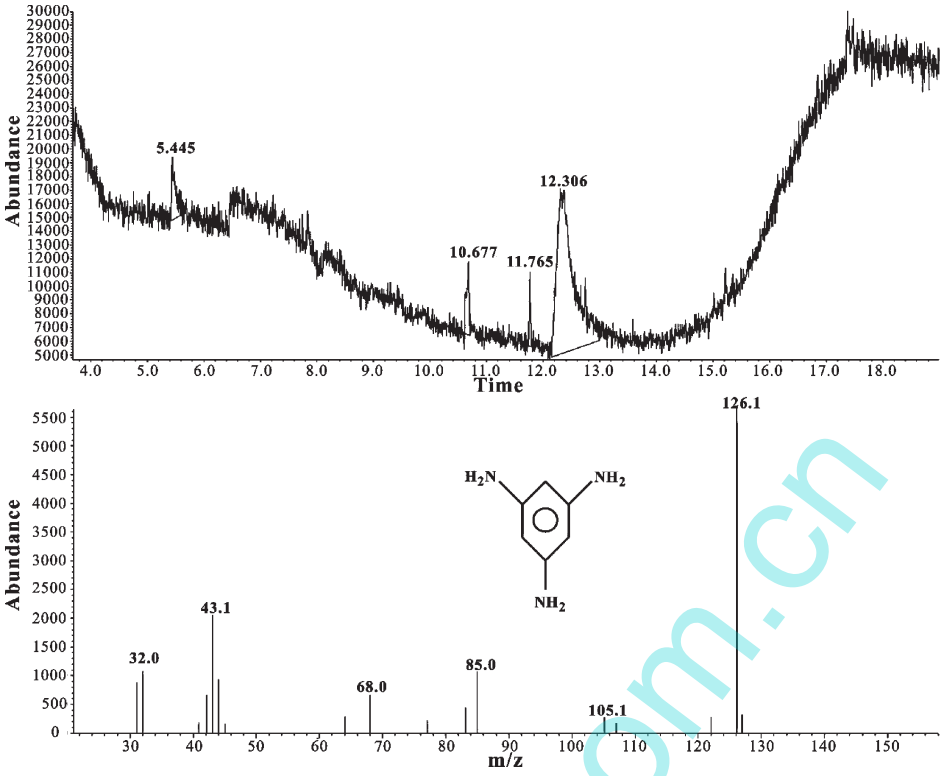

Figure 7. GC-MS spectrum for melamine detection (5 ppm) in 0.1 M H_2SO_4 solution.

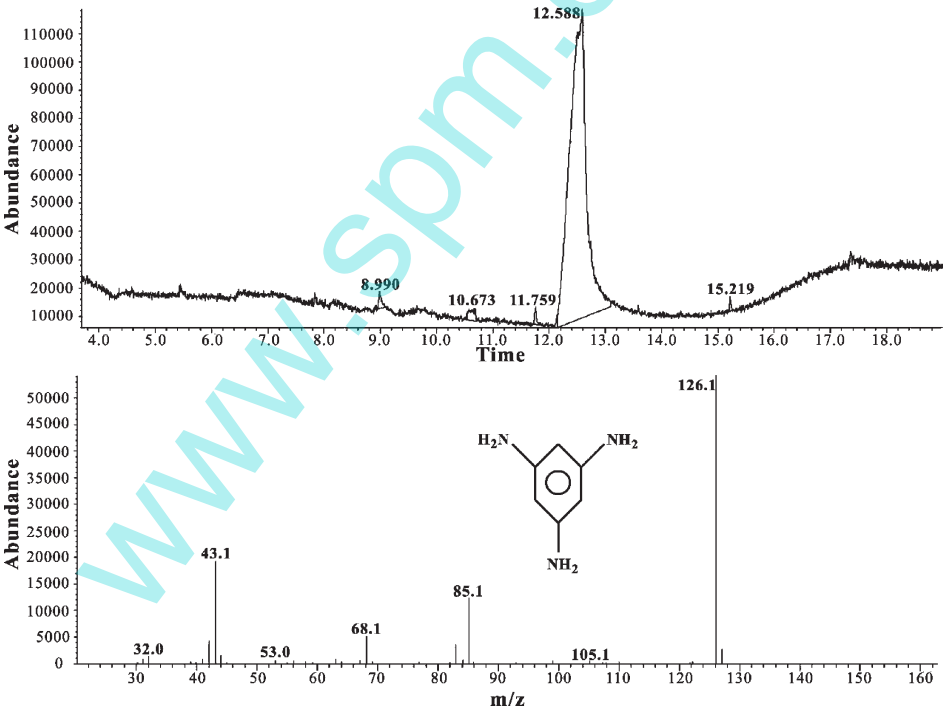

Figure 8. GC-MS spectrum for melamine detection (5 ppm) in milk powder sample.

DPV voltammograms of spiked melamine in human urine sample using poly GE. Here we can observe the well-separated anodic oxidation peaks for uric acid (UA) (0.76 V) and spiked melamine (1.08 V). The peak separation between UA and melamine was found as 0.32 V. This peak separation is sufficient for the detection of melamine in the human urine sample. SET-B in **Figure 6** shows the overlay of various concentrations (a−g) of melamine detection in pH 1 H_2SO_4 using poly GE. Here the amplified current obtained for the urine sample is compared with melamine detection in pH 1 H_2SO_4. This is because of the matrix effect of urine sample. However, for the increasing concentrations of melamine in urine sample the anodic peak clearly increases at the poly GE.

The interesting factor here is the selective detection of melamine in the presence of uric acid. The inset of **Figure 6** shows the current versus calibration plot of melamine detection in human urine sample. From this calibration plot the linear regression equation for the melamine detection in urine sample

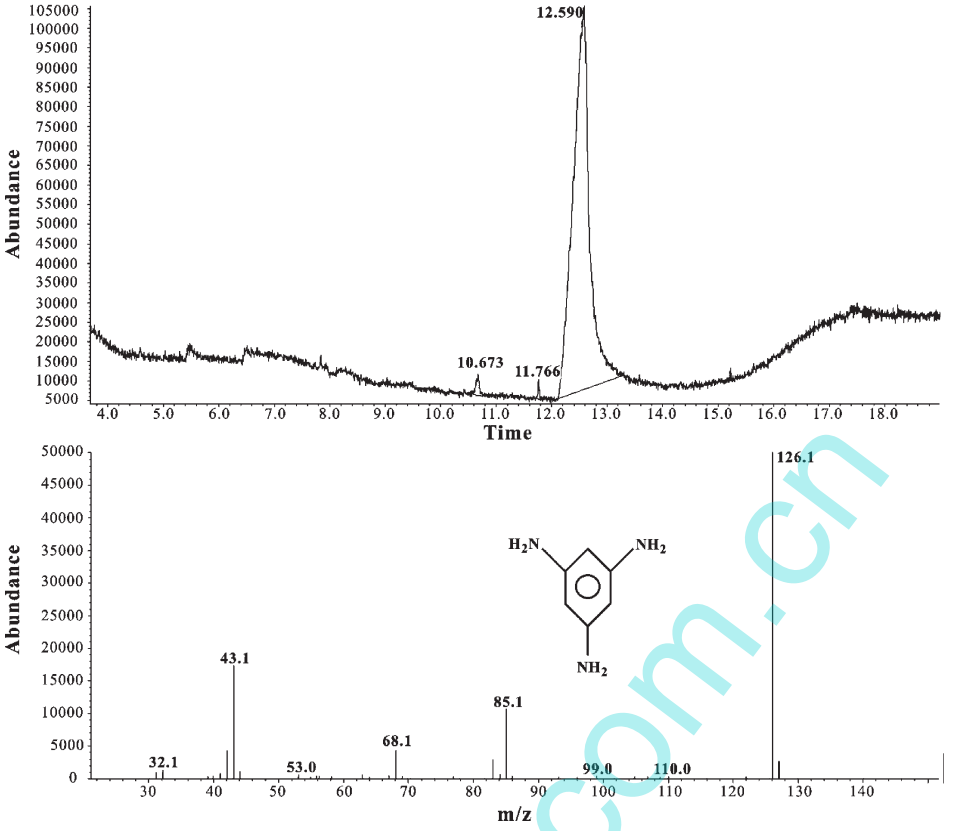

Figure 9. GC-MS spectrum for melamine detection (5 ppm) in urine sample.

Table 1. Comparison Table for Melamine Detection[a]

sample	analytical method	material	melamine detection	ref
1	LC-UV, GC-MSD	soil	2−80 ppb	*11*
2	HPLC-MS/MS	edible hog tissue	50−2000 ng/mL	*5*
3	HPLC	cereal flours	5−500 ppm	*6*
4	HPLC	poultry meats and eggs	0.2−0.7 ppm	*9*
5	reversed phase LC-MS	liquid milk and dry milk powder	0.1 ng/g (LOQ)	*26*
6	CZE-DAD	dairy products, fish and fish feeds	0.05−10 μg/mL	*27*
		water	2.5−1000 ng/mL	
		liquid milk	30−5000 ng/mL	
7	LTP/MS/MS	synthetic urine	20−5000 ng/mL	*28*
		milk powder	10−2500 ng/g	
		soy milk powder	20−3000 ng/g	
8	oxidized poly GE	tainted milk powder	0.06−0.85 ppm	this work
		human urine	0.05−0.44 ppm	

[a] LOQ, limit of quantification; LC-UV, liquid chromatography−ultraviolet; GC-MSD, gas chromatography−mass selective detection; HPLC-MS/MS, high-performance liquid chromatography−tandem mass spectroscopy; CZE-DAD, capillary zone electrophoresis with diode array detection; LTP/MS/MS, low-temperature plasma probe combined with tandem mass spectrometry.

has been found as I_{pa} (μA) = 21.75C (ppm) + 19.17, R^2 = 0.990. All of these results clearly validate the capability of the proposed electrode for the detection of melamine in human urine sample.

In the next step GC-MS was successfully employed for the detection of melamine (5 ppm) in the above proposed samples (0.1 M H_2SO_4, milk powder, urine sample) (**Figures 7−9**).

Here the real samples have been prepared as mentioned before for the electrochemical analysis. For all three types of samples GC-MS clearly exhibits the spectrum for detection of melamine. However, a few low signal interferences were obtained in both milk and urine samples. Four characteristic ions were found for melamine detection in the corresponding samples at *m*/*z* 126.1, 85.0, 68.0, and 43.1 (*25*). Therefore, the proposed electrochemical detection method could be utilized along with the other separation techniques for the detection and determination of melamine.

Table 1 shows the previous literature reports of melamine detection. In this table, we have compared the important previous literature reports for melamine detection. Compared with these rapid analytical techniques, electrochemical detection is quite interesting for the detection of melamine. At the same time, direct analytical techniques are more favorable compared with electrochemical detection because we propose the electroanalytical method based on the adsorption signal of the melamine on the electrode surface. Simply, the proposed electrochemical detection could be utilized along with verification by other analytical techniques. On the basis of this comparison study, we propose that this method could be applied for the detection of melamine in real samples.

ACKNOWLEDGMENT

We acknowledge Evergreen Chemical Industrial Corp. (R&D division), Taiwan (ROC), for their timely support in utilizing GC-MS.

LITERATURE CITED

(1) Xin, H.; Stone, R. Tainted milk scandal: Chinese probe unmasks high-tech adulteration with melamine. *Science* **2008**, *322*, 1310–1311.
(2) Yang, V. L.; Batlle, D. Acute renal failure from adulteration of milk with melamine. *Sci. World J.* **2008**, *8*, 974–975.
(3) Hirt, R. C.; King, F. T.; Schmitt, R. G. Detection and estimation of melamine in wet-strength paper by UV spectrophotometry. *Anal. Chem.* **1954**, *26*, 1273–1274.
(4) Swann, M. H.; Esposito, G. G. Detection of urea, melamine, isocyanate, and urethan resins. *Anal. Chem.* **1958**, *30*, 107–109.
(5) Filigenzi, M. S.; Tor, E. R.; Poppenga, R. H.; Aston, L. A.; B. Puschner, B. The determination of melamine in muscle tissue by liquid chromatography/tandem mass spectrometry. *Rapid Commun. Mass Spectrom.* **2007**, *21*, 4027–4032.
(6) Ehling, S.; Tefera, S.; Ho, I. P. High-performance liquid chromatographic method for the simultaneous detection of the adulteration of cereal flours with melamine and related triazine by-products ammeline, ammelide, and cyanuric acid food additives and contaminants. *Food Addit. Contam.* **2007**, *24*, 1319–1325.
(7) Valencia, R. M.; Ceballos-Magaña, S. G.; DanielRosales-Martinez, D.; Gonzalo-Lumbreras, R.; Santos-Montes, A.; Cubedo-Fernandez-Trapiella, A.; Izquierdo-Hornillos, R. C. Method development and validation for melamine and its derivatives in rice concentrates by liquid chromatography. Application to animal feed samples. *Anal. Bioanal. Chem.* **2008**, *392*, 523–531.
(8) Onoa, S.; Funatoa, T.; Inouea, Y.; Munechika, T.; Yoshimura, T.; Morita, H.; Rengakuji, S.-I.; Shimasaki, C. Determination of melamine derivatives, melame, meleme, ammeline and ammelide by high-performance cation-exchange chromatography. *J. Chromatogr., A* **1998**, *815*, 197–204.
(9) Chou, S. S.; Hwang, D.-F.; Lee, H.-F. High performance liquid chromatographic determination of cyromazine and its derivative melamine in poultry meats and eggs. *J. Food Drug Anal.* **2003**, *11*, 290–295.
(10) Sancho, J. V.; Ibáñez, M.; Grimalt, S.; Pozo, Ó.; Hernández, F. Residue determination of cyromazine and its metabolite melamine in chard samples by ion-pair liquid chromatography coupled to electro spray tandem mass spectrometry. *Anal. Chim. Acta* **2005**, *530*, 237–243.
(11) Yokley, R. A.; Mayer, L. C.; Rezaaiyan, R.; Manuli, M. E.; Cheung, M. W. Analytical method for the determination of cyromazine and melamine residues in soil using LC-UV and GC-MSD. *J. Agric. Food Chem.* **2000**, *48*, 3352–3358.
(12) Lin, M.; He, L.; Awika, J.; Yang, L.; Ledoux, D. R.; Li, H.; Mustapha, A. Detection of melamine in gluten, chicken feed, and processed foods using surface enhanced Raman spectroscopy and HPLC. *J. Food Sci.* **2008**, *73*, T129–T134.
(13) Thanhvo, T. D.; Himmelsbach, M.; Haunschmidt, M.; Buchberger, W.; Schwarzinger, C.; Klampfl, C. W. Improved analysis of melamine−formaldehyde resins by capillary zone electrophoresis−mass spectrometry using ion-trap and quadrupole-time-of-flight mass spectrometers. *J. Chromatogr., A* **2008**, *1213*, 83–87.
(14) Cook, H. A.; Klampfl, C.; Buchberger, W. Analysis of melamine resins by capillary zone electrophoresis with electrospray ionization mass spectrometric detection. *Electrophoresis* **2005**, *26*, 1576–1583.
(15) Schmidt, V. M.; Pastore, E. Electrochemical reactions of ethyne adsorbed on polycrystalline Au electrodes. *J. Phys. Chem.* **1995**, *99*, 13247–13256.
(16) Zelenay, P.; Rice-Jackson, L. M.; Wieckowski, A. Adsorption of pyridine on polycrystalline gold electrode studied by radioactive-labeling method. *Langmuir* **1990**, *6*, 974–979.
(17) Ferapontova, E. E.; DomÌnguez, E. Direct electrochemical oxidation of DNA on polycrystalline gold electrodes. *Electroanalysis* **2003**, *15*, 629–634.
(18) Mura, M.; Martsinovich, N.; Kantorovich, L. Theoretical study of melamine superstructures and their interaction with the Au(111) surface. *Nanotechnology* **2008**, *19*, 465704–465717.
(19) Perdigo, L. M. A.; Perkins, E. W.; Ma, J.; Staniec, P. A.; Rogers, B. L.; Champness, N. R.; Beton, P. H. Bimolecular networks and supramolecular traps on Au (111). *J. Phys. Chem. B* **2006**, *110*, 12539–12542.
(20) Staniec, P. A.; Perdigao, L. M. A.; Saywell, A.; Champness, N. R.; Beton, P. H. Hierarchical organisation on a two-dimensional supramolecular network. *ChemPhysChem* **2007**, *8*, 2177–2181.
(21) Silly, F.; Shaw, A. Q.; Castell, M. R.; Briggs, G. A. D.; Mura, M.; Martsinovich, N.; Kantorovich, L. Melamine structures on the Au(111) Surface. *J. Phys. Chem. C* **2008**, *112*, 11476–11480.
(22) Kazuki, A.; Takako, A.; Noriko, T.; Kayo, A.; Takeyoshi, O.; Fusao, K.; Koichi, T.; Takeo, O. Multiple voltammetric waves for reductive desorption of cysteine and 4-mercaptobenzoic acid monolayers self-assembled on gold substrates. *Phys. Chem. Chem. Phys.* **2003**, *5*, 3758–3761.
(23) Gonzalo, G.; Rodŕguez, J. L.; Lacconi, G. I.; Pastor, E. Spectroscopic investigation of the adsorption and oxidation of thiourea on polycrystalline Au and Au(111) in acidic media. *Langmuir* **2004**, *20*, 8773–8780.
(24) Borkowska, Z.; Tymosiak-Zielinska, A.; Shul, G. Electrooxidation of methanol on polycrystalline and single crystal gold electrodes. *Electrochim. Acta* **2004**, *49*, 1209–1220.
(25) Xu, X.-X.; Ren, Y.-P.; Zhu, Y.; Cai, Z.-X.; Han, J.-L.; Huang, B.-F.; Zhu, Y. Direct determination of melamine in dairy products by gas chromatography/mass spectrometry with coupled column separation. *Anal. Chim. Acta* **2009**, *650*, 39–43.
(26) Qing, W. Q.; Xin, F. K.; Wei, S.; Qiang, R. H.; Rong, Z.; Hui, S. C. Highly sensitive detection of melamine based on reversed phase liquid chromatography mass spectrometry. *Chinese Sci. Bull.* **2009**, *54*, 732–737.
(27) Yan, N.; Zhou, L.; Zhu, Z.; Chen, X. Analytical method for the determination of cyromazine and melamine residues in soil using LC-UV and GC-MSD. *J. Agric. Food Chem.* **2009**, *57*, 807–811.
(28) Huang, G. M.; Yang, Z. O.; Cooks, R. G. High-throughput trace melamine analysis in complex mixtures. *Chem. Commun.* **2009**, *5*, 556–558.

Received for review August 20, 2009. Accepted March 22, 2010. This work was supported by grants from the National Science Council (NSC) of Taiwan (ROC).